NPG Asia Materials (2013) 5, e44; doi:10.1038/am.2013.7

www.nature.com/am

ORIGINAL ARTICLE

Biodistribution and pulmonary toxicity of intratracheally instilled graphene oxide in mice

Bo Li[1,2], Jianzhong Yang[1], Qing Huang[1], Yi Zhang[1], Cheng Peng[1], Yujie Zhang[1], Yao He[1,3], Jiye Shi[1,4], Wenxin Li[1], Jun Hu[1] and Chunhai Fan[1]

Graphene and its derivatives (for example, nanoscale graphene oxide (NGO)) have emerged as extremely attractive nanomaterials for a wide range of applications, including diagnostics and therapeutics. In this work, we present a systematic study on the *in vivo* distribution and pulmonary toxicity of NGO for up to 3 months after exposure. Radioisotope tracing and morphological observation demonstrated that intratracheally instilled NGO was mainly retained in the lung. NGO could result in acute lung injury (ALI) and chronic pulmonary fibrosis. Such NGO-induced ALI was related to oxidative stress and could effectively be relieved with dexamethasone treatment. In addition, we found that the biodistribution of ^{125}I-NGO varied greatly from that of ^{125}I ions, hence it is possible that nanoparticulates could deliver radioactive isotopes deep into the lung, which might settle in numerous 'hot spots' that could result in mutations and cancers, raising environmental concerns about the large-scale production of graphene oxide.
NPG Asia Materials (2013) **5,** e44; doi:10.1038/am.2013.7; published online 5 April 2013

Keywords: biodistribution; graphene oxide; intratracheal instillation; mice; pulmonary toxicity

INTRODUCTION

Graphene is a recently discovered, two-dimensional nanomaterial with a one-atom thickness.[1] Graphene and its derivatives (for example, nanoscale graphene oxide (NGO)) have shown unique thermal, mechanical and electronic properties that have attracted tremendous attention in applications including nanocomposites and transistors, as well as diagnostics and therapeutics.[2–4] In particular, water-dispersible NGO has proven to be a promising nanocarrier for drug delivery. Hence, it is critically important to address the safety issue of NGO before its *in vivo* biomedical application.

The lung is the primary organ invaded by nanomaterials because of the communication of this organ with the outside atmosphere through the respiratory tract. In addition, nanoparticles (<100 nm) have previously been found to deposit mainly in the lungs.[5] Therefore, intratracheal instillation was used to investigate the biodistribution and pulmonary toxicity of NGO in C57BL/6 mice for up to 3 months. We employed radioisotope tracing and conventional evaluation system to study the *in vivo* absorption, distribution, metabolism, excretion and toxicity of NGO in mice. Our finding on the apparent discrepancy in biodistribution of ^{125}I-NGO with iodine-125 ions also raises potential concerns on the identification of target organs and critical effects upon nuclear radiation exposure.

MATERIALS AND METHODS

NGO was synthesized from natural graphite by oxidation with $H_2SO_4/KMnO_4$ according to a modified Hummers method.[6] The resulting NGO was characterized by Fourier transform infrared spectroscopy, Raman spectroscopy, atomic force microscopy, scanning electron microscopy and transmission electron microscopy.

SPECT imaging was used to dynamically assess the *in vivo* distribution of ^{125}I-NGO within 60 min. KunMing mice ($n=2$) were anesthetized with an intraperitoneal injection of 50 mg kg^{-1} pentobarbital sodium (10 mg ml^{-1}; Sigma, St. Louis, MO, USA) and placed in a supine position on a board. After 1.85×10^6 Bq ^{125}I-NGO and Na^{125}I in a 0.1-ml volume were intratracheally instilled into the mice, respectively, whole-length dynamic imaging was immediately performed with a gamma camera (Elscint Apex SP-6, Elscint Ltd., Haifa, Israel) at 5, 10, 20, 30, 40, 50 and 60 min. A count for each time point was collected for 100 s in the anterior and posterior positions with an energy window of $\approx$30 keV and a matrix of 73×73.

To determine the *in vivo* distribution of NGO in more detail, each KunMing mouse was exposed to 100 μl of a ^{125}I-NGO aqueous solution via intratracheal instillation. The animals were killed at different time points. The blood, urine and major organs, including thyroid gland, heart, lungs, liver, spleen, kidneys, stomach (emptied), small intestine (full) and large intestine (full), were collected, and the ^{125}I activity was counted using a γ-detector. The distribution of ^{125}I-NGO in the blood and each organ was represented by the percentage of the exposed dose (sample activity/total activity dosed, %ED). The concentration of ^{125}I-NGO in the urine was represented by the percentage of the exposed dose per gram (%ED per g).

[1]Laboratory of Physical Biology, Shanghai Institute of Applied Physics, Chinese Academy of Sciences, Shanghai, China; [2]Department of Human Anatomy, Norman Bethune College of Medicine, Jilin University, Changchun, China; [3]Functional Nano and Soft Materials Laboratory (FUNSOM), Soochow University, Suzhou, China and [4]UCB Pharma, Slough, UK
Correspondence: Professor Q Huang or Professor C Fan , Laboratory of Physical Biology, Shanghai Institute of Applied Physics, Chinese Academy of Sciences, PO Box 800-204, Shanghai 201800, China.
E-mail: huangqing@sinap.ac.cn or fchh@sinap.ac.cn
Received 8 November 2012; revised 22 December 2012; accepted 30 January 2013

Considering the potential threat to workers posed by accidental industrial exposure to NGO during production and transportation, the mice were intratracheally instilled with high-dosage NGO to investigate its acute and chronic pulmonary toxicity. To elucidate the dosage-related pulmonary responses induced by NGO, groups of C57BL/6 mice were intratracheally instilled with 0, 1, 5 or 10 mg kg^{-1} NGO (using 0, 0.2, 1 and 2 mg ml^{-1} suspension solutions, respectively) and terminated at 24 h post exposure (see Supplementary Information, Supplementary Table. S1). To assess the time-related pulmonary responses induced by NGO, groups of mice were instilled intratracheally with 10 mg kg^{-1} NGO (using a 2 mg ml^{-1} suspension solution) and terminated at 0 h, 24 h, 48 h, 72 h and 1 week after the intratracheal instillation, respectively. The evaluation system was composed of the following: (1) the bronchoalveolar lavage (BAL) fluid biomedical index, (2) lung wet/dry weight ratio, (3) BAL fluid differential cell counting, (4) lung histopathological evaluation and (5) an oxidative stress assay.

To evaluate the chronic pulmonary responses induced by NGO, groups of mice were instilled intratracheally with 10 mg kg^{-1} NGO (using a 2 mg ml^{-1} suspension solution) and terminated at 1 and 3 months after the intratracheal instillation, respectively. The histopathological characteristics of the chronic pulmonary lesions induced by NGO were assessed by standard hematoxylin-eosin and Masson trichrome staining.

To determine the therapeutic effect of dexamethasone (DEX) on NGO-induced acute lung injury (ALI), 45 C57BL/6 mice were randomly divided into three groups ($n = 15$ in each group): Milli-Q water group, NGO group and NGO + DEX group. The mice in both the NGO and the NGO + DEX groups were intratracheally instilled with 10 mg kg^{-1} NGO (using a 2 mg ml^{-1}

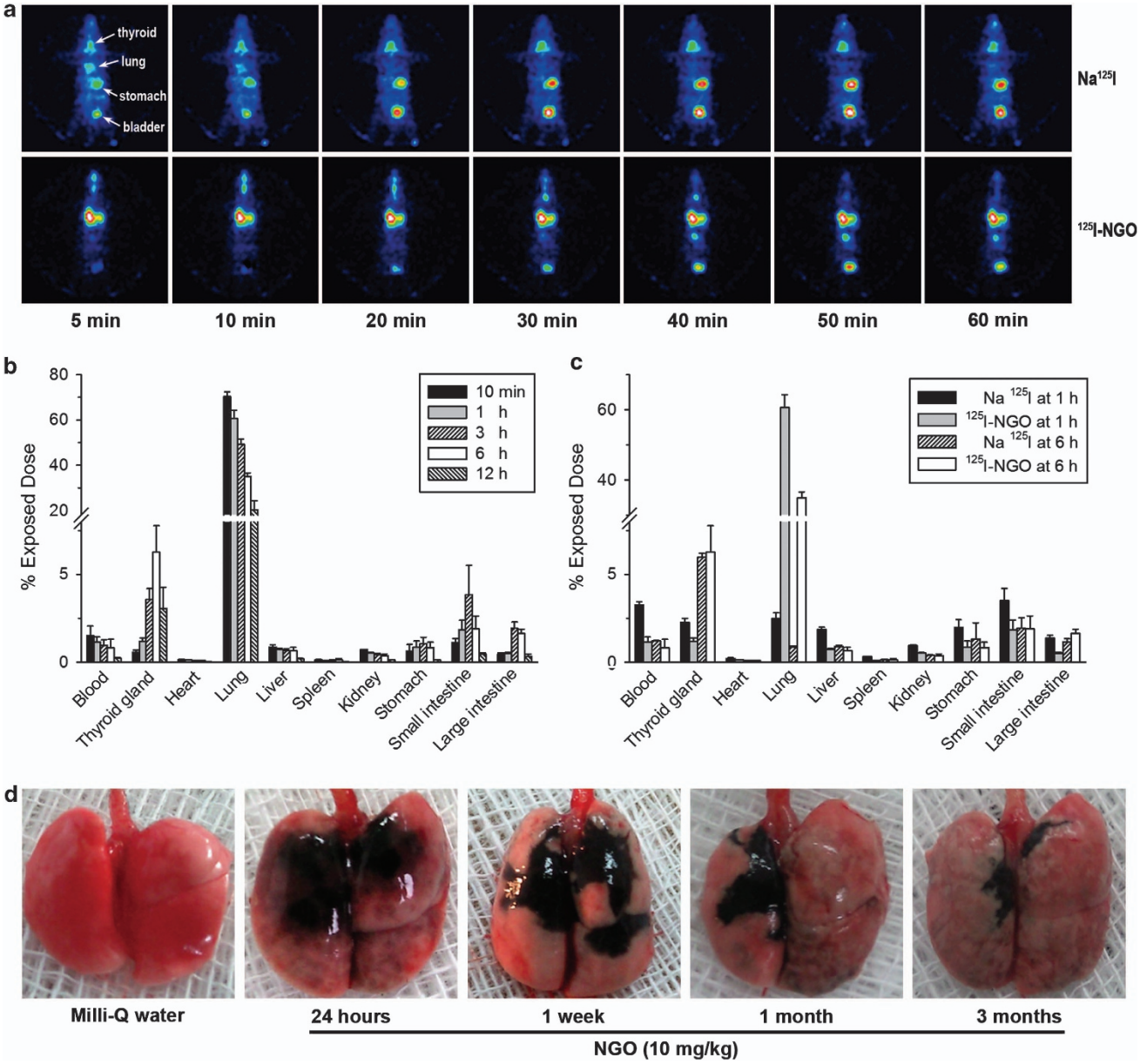

Figure 1 Biodistribution of NGO after intratracheal instillation. (**a**) SPECT images of mice at several time points after intratracheal instillation with ^{125}I-NGO or Na^{125}I. (**b**) Distribution of ^{125}I-NGO in the blood and major organs of mice at five different time points. $N = 5$ in each group. Values are presented as the mean ± s.e.m. (**c**) Comparison of Na^{125}I and ^{125}I-NGO distribution in mice at 1 and 6 h after intratracheal instillation. $N = 5$ in each group. Values are presented as the mean ± s.e.m. (**d**) The morphological observation of the lungs from mice instilled with Milli-Q water or 10 mg kg^{-1} NGO. The dorsal view shows the distribution of NGO (black region).

suspension solution). Meanwhile, the mice in the Milli-Q water group received the same volume of Milli-Q water and the same manipulations. Immediately after instillation, the mice in the NGO + DEX group received an intraperitoneal injection of 5 mg kg^{-1} DEX (dissolved in 0.1 ml 0.9% saline), whereas the mice in the other two groups received the same volume of 0.9% saline and the same manipulations. Mice from all three groups were terminated at 24 h after the intratracheal instillation. The BAL fluid biomedical index, the BAL fluid differential cell counting, the lung wet/dry weight ratio and the histopathological evaluation were determined (see Supplementary Information, Supplementary Method).

RESULTS AND DISCUSSION

^{125}I was selected for *in vivo* tracking of NGO because of its easy labeling and simple biosampling.[7] Our results indicate that ^{125}I-NGO primarily remains in the lung after intratracheal instillation. SPECT images showed a very bright spot located in the lungs of mouse instilled with ^{125}I-NGO at each time point. Furthermore, the brightness in the lung maintained almost the same levels for 60 min after exposure (Figure 1a). The high retention of ^{125}I-NGO in the lung observed in these images was also supported by the values of radioactivity for organs (Figure 1b). The radioactivity in the lung was ~70.3% of the exposed dose at 10 min. Although the radioactivity gradually decreased over time, 20.2% of the exposed dose remained after 12 h. Interestingly, we observed the presence of radioactivity, albeit at a small level (<5%), in other organs, such as the liver and the small and large intestines. Their radioactivity increased over the first several hours, suggesting that NGO may pass through the air–blood barrier into blood and be delivered to other organs. In addition, the presence of radioactivity in the thyroid gland may have arisen from the small amounts of ^{125}I ions released from the ^{125}I-NGO conjugate.[8]

The biodistribution of Na^{125}I was compared with that of ^{125}I-NGO to evaluate the *in vivo* stability of ^{125}I-NGO (Figures 1a and c). The significant differences in the biodistribution of ^{125}I-NGO and Na^{125}I demonstrated that ^{125}I-NGO was stable *in vivo* and that the results of the distribution of ^{125}I-NGO were accurate and reliable. However, the apparent discrepancy in the biodistribution of ^{125}I-NGO and ^{125}I ions raises potential concerns about the identification of target organs and the critical effects of the nuclear radiation exposure.[9–11]

The clearance of NGO was evaluated by using radioisotope tracing and morphological observation. SPECT images showed that the radioactivity intensity in the bladder of mouse instilled with

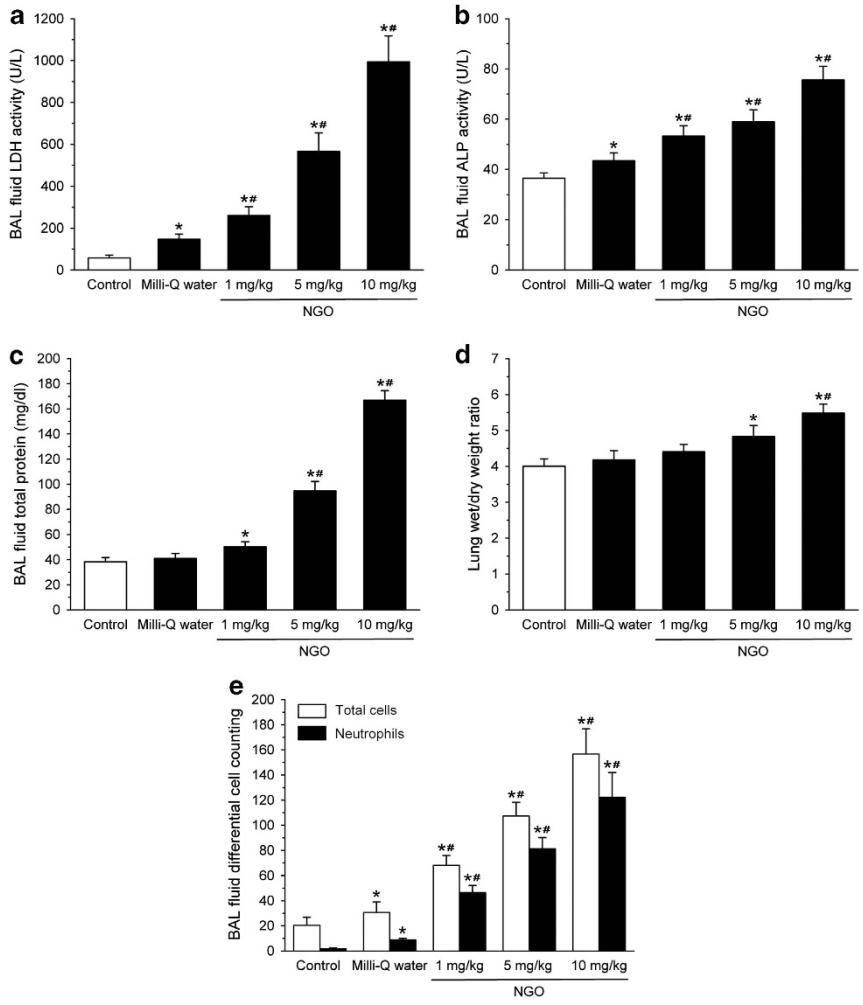

Figure 2 NGO causes dosage-dependent ALI characterized chiefly by cell injury, lung edema and neutrophil infiltration. (**a**–**e**) BAL fluid LDH (**a**), ALP (**b**) and total protein (**c**) assays were performed to determine the level of cell injury. The lung wet/dry weight ratio (**d**) was used to evaluate the severity of lung edema. BAL fluid differential cell counting (**e**) was used to evaluate the number and types of migrated cells. The symbol '*' indicates values that differed significantly from the control group at $P<0.05$; the symbol '#' indicates values that differed significantly from the Milli-Q water group at $P<0.05$. $N=5$ in each group. Values are presented as the mean ± s.e.m.

^{125}I-NGO gradually increased within 60 min (Figure 1a). The relatively high values of concentration of ^{125}I-NGO in urine were observed within 6 h (see Supplementary Information, Supplementary Figure S1). These results indicate that NGO sheets with small sizes can penetrate the alveolar–capillary barrier into blood and be quickly eliminated by a renal route. The long-term fate of NGO in the lung was examined using morphological changes of excised lungs. Lungs from mice treated with NGO exhibited a black discoloration that reflected NGO deposition in lung tissue (Figure 1d). The regions of black discoloration on the lung surface were gradually reduced from 24 h to 3 months after instillation, implying that NGO is slowly cleared from the lungs. Histopathological observation showed that there was an obvious accumulation of alveolar macrophages laden with NGO in the bronchial lumen at 3 months (see Supplementary Information, Supplementary Figure S2). This observation suggests that NGO is taken up and cleared by alveolar macrophages, and the alveolar macrophages may be eliminated in the sputum from the body through mucociliary clearance or by other mechanisms.[12,13] NGO may also be gradually degraded over time by the oxidative metabolic pathways.[10] However, both the presence of black discoloration on the lung surface after 3 months (Figure 1d) and the histopathological observation (Supplementary Figure S2) indicate incomplete clearance of NGO.

The pulmonary responses induced by nanoparticles were closely related to their dispersion in the lung.[14] We found that the procedures of administration are important for both the distribution of NGO and the mortality of mice. When syringes were prefilled with 100 μl of air before suctioning up the NGO, NGO was well dispersed immediately after instillation, resulting in minimal mortality from mechanical blockage by nanomaterials in the airways (data not shown).

Histopathological evaluation of the lung tissue was performed after 0 h, 24 h, 48 h, 72 h and 1 week (see Supplementary Information, Supplementary Figure S3). Immediately after intratracheal instillation of 10 mg kg^{-1} NGO, NGO had mainly adhered to the inner surfaces of the bronchial and alveolar walls. There was no formation of large aggregates blocking the bronchial lumina and alveolar spaces, and a good dispersion pattern was observed. Subsequently, NGO began to aggregate, and this aggregation was accompanied by an obvious pulmonary inflammatory response. Large agglomerates of NGO were clearly visualized after 1 week.

We performed assays of cell injury, lung edema and neutrophil infiltration to evaluate the acute pulmonary responses induced by NGO. The BAL fluid biomedical index, which includes lactate dehydrogenase (LDH) activity, alkaline phosphatase (ALP) activity and total protein concentration, was determined to measure the level of cell injury. After 24 h, dosage-dependent increases in the activities of LDH and ALP and the levels of total protein in the BAL fluid were observed (Figures 2a–c). LDH and ALP are indicators of cell injury, and the increase in ALP activity is particularly suggestive of type II

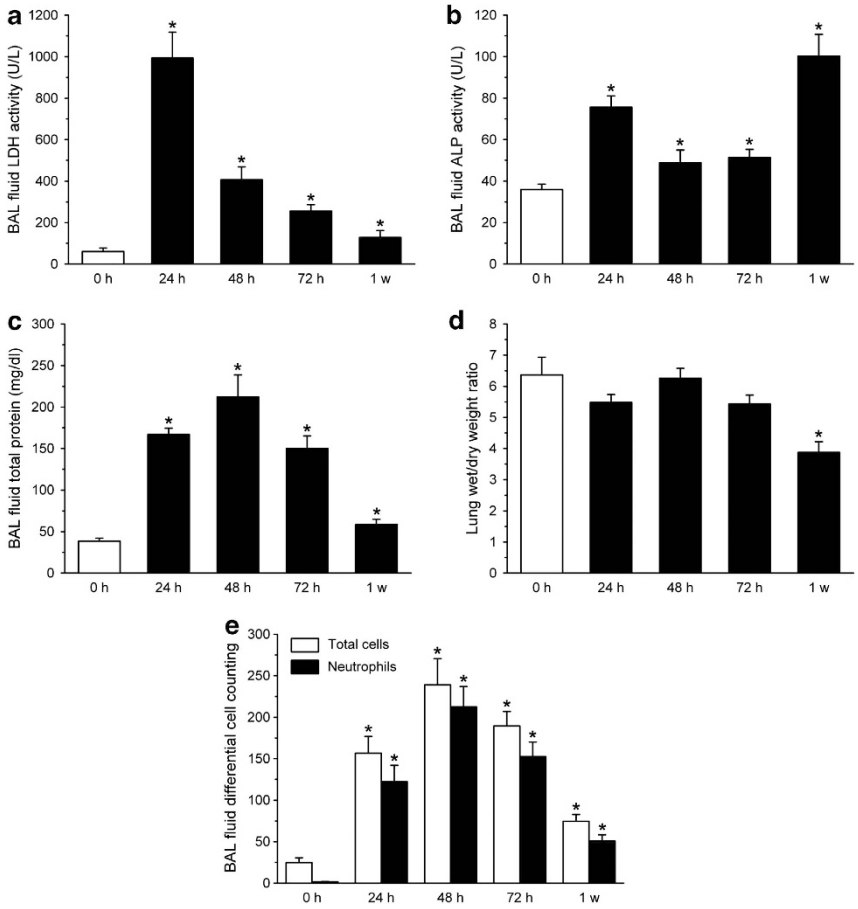

Figure 3 NGO-induced ALI is progressive. (**a**–**e**) BAL fluid LDH (**a**), ALP (**b**) and total protein (**c**) were performed to determine the level of cell injury. The lung wet/dry weight ratio (**d**) was used to evaluate the severity of lung edema. BAL fluid differential cell counting (**e**) was used to evaluate the number and types of migrated cells. The symbol '*' indicates values that differed significantly from the 0 h group at $P<0.05$. $N=5$ in each group. Values are presented as the mean ± s.e.m.

lung epithelial cell toxicity. The increase in the total protein concentration in the BAL fluid implied the enhanced permeability of vascular proteins into the alveolar regions; this effect could have arisen from the breakdown of the integrity of the alveolar–capillary barrier.

Cell injury in the lung is often associated with lung edema, which is the result of the leakage of fluid from the capillaries into the interstitial and alveolar spaces and the loss of the lung's ability to pump fluid out of the airspace. Indeed, we found that NGO led to an increase in the lung wet/dry weight ratio in a dosage-dependent manner (Figure 2d); this ratio is an indicator of the severity of the lung edema.

We also found that the cells recovered from the BAL fluid were mainly neutrophils (polymorphonuclear leukocytes) under the stimulation with NGO (Figure 2e). The dosage-dependent increase in the number of neutrophils suggests the occurrence of neutrophil infiltration. Recruitment of neutrophils into the lung is a key event in the early development of ALI, as previously demonstrated in neutropenic animals and humans.[15,16]

Lung histopathological changes also varied with the dosage of instilled NGO (see Supplementary Information, Supplementary Figure S4). Compared with the control group instilled with Milli-Q water, the lungs of the 1 and 5 mg kg^{-1} NGO groups exhibited mild to moderate interstitial edema, neutrophil infiltration and alveolar septa thickening. Furthermore, the alveoli in the 10 mg kg^{-1} NGO group exhibited the presence of protein-rich fluid (pulmonary parenchymal edema) and neutrophil infiltration accompanied by diffuse congestion and hemorrhage. Overall, NGO resulted in ALI, a clinical syndrome characterized by an excessive inflammatory response to both pulmonary and extrapulmonary stimuli that ultimately leads to a disruption of alveolar–capillary integrity with severe consequences for pulmonary gas exchange.[17]

Given that NGO caused ALI at 24 h post exposure, we examined the time-dependent pulmonary responses induced by NGO. LDH and ALP activities were elevated at 24 h and then decreased (Figures 3a and b), suggesting that NGO induces early severe cell damage. The peaks of BAL fluid total protein, lung wet/dry weight ratio and BAL fluid differential cell counts occurred at 48 h, suggesting that this is the time point of the most severe disruption of the alveolar–capillary interface, lung edema and neutrophil infiltration (Figures 3c–e). Moreover, the diffuse lung edema with protein-rich fluid, extensive hemorrhage and significant changes in alveolar architecture were clearly observed 48 h after instillation (see Supplementary Information, Supplementary Figure S3). These results indicate that NGO-induced ALI is progressive; it exhibits its greatest severity at 48 h and then is alleviated. Furthermore, the fibroproliferation and

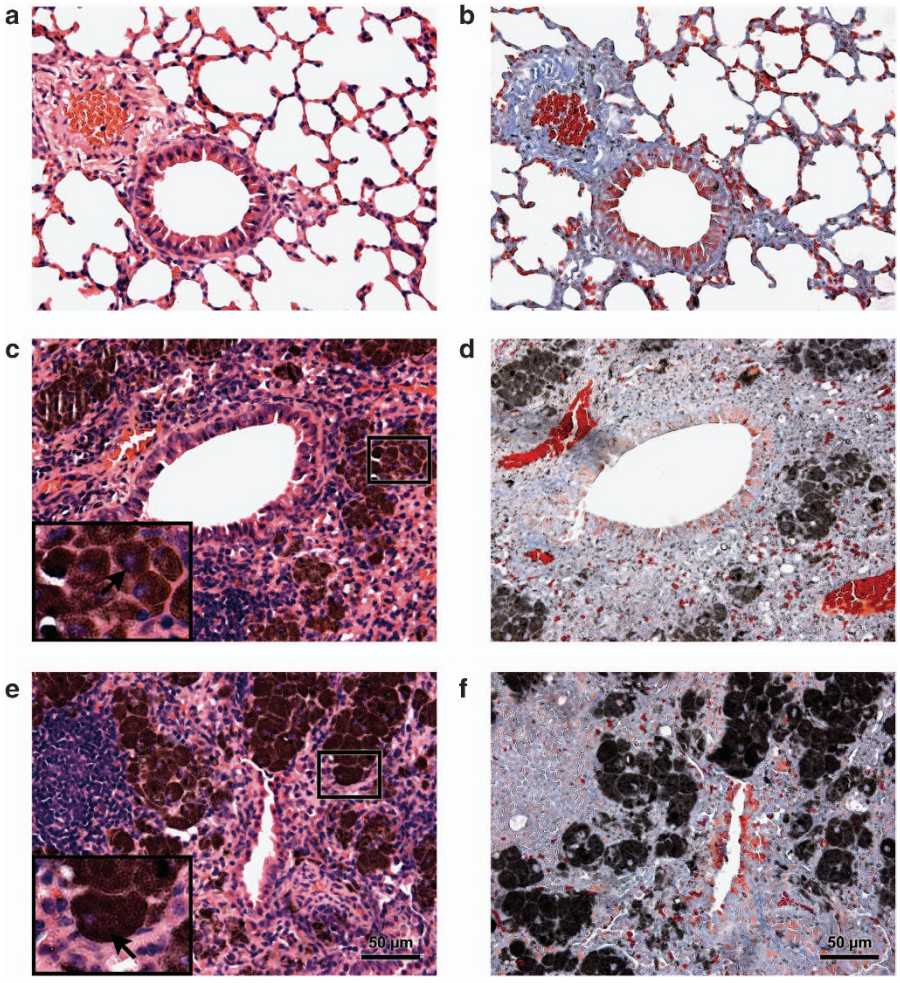

Figure 4 Chronic pulmonary lesions induced by NGO. Hematoxylin-eosin (**a**, **c**, **e**) and Masson trichrome (**b**, **d**, **f**) staining of lung tissues from the mice instilled with Milli-Q water (**a**, **b**)or 10 mg kg^{-1} NGO (**c**–**f**). NGO induced diffuse pulmonary fibrosis at 1 month (**c**, **d**) and 3 months (**e**, **f**). The black arrows indicate NGO. All images are shown at $\times$400 magnification with a 50-μm scale bar; insets are shown at $\times$1000 magnification.

organization of lung tissue at 1 week indicates the emergence of lung fibrosis (see Supplementary Information, Supplementary Figure S3).

The histopathological characteristics of the chronic pulmonary lesions induced by NGO were assessed by standard hematoxylin-eosin and Masson trichrome staining (Figure 4). Histopathological analysis clearly showed a consolidation of the lung and an accumulation of alveolar macrophages laden with NGO at 1 and 3 months post exposure (Figures 4c and e). Meanwhile, there was obvious collagen deposition and numerous inflammatory cells surrounding the alveolar macrophages. Compared with the 1-month group, the bronchial lumina in the 3-month group had become narrow and even closed, suggesting the further exacerbation of the fibrotic response. These results indicate that NGO induced diffuse pulmonary fibrosis over a longer term.

Because the inflammatory responses caused by nanomaterials are often associated with oxidative stress,[18,19] we examined the degree of oxidative stress in the lung by measuring the levels of two antioxidants, superoxide dismutase (SOD) and glutathione peroxidase (GSH-PX). We observed a dosage-dependent decrease in SOD and GSH-PX activities in the lung tissue (Figures 5a and c). In addition, the SOD and GSH-PX activities were progressively reduced after the exposure to NGO, reaching a minimum at 48 h, followed by an elevation until 1 week (Figures 5b and d). These data suggest that oxidative stress has a significant role in NGO-induced ALI.

DEX treatment is regarded as a good choice for the treatment of ALI/acute respiratory distress syndrome.[20] Therefore, we evaluated the therapeutic effect of DEX on the ALI induced by NGO at 24 h. LDH and ALP activities and total protein level in BAL fluid in the NGO + DEX group were significantly decreased compared with the NGO group (Figures 6a–c). This result suggests that the DEX treatment attenuated the NGO-induced cell injury. Meanwhile, the lung wet/dry ratio and the number of neutrophils in BAL fluid in the NGO + DEX group were significantly decreased compared with the NGO group (Figures 6d and e), suggesting that DEX alleviated the lung edema and neutrophil infiltration induced by NGO. Histopathological observation further verified the effect of DEX treatment (see Supplementary Information, Supplementary Figure S5). At 24 h in the NGO group, the alveoli exhibited more protein-rich fluid and more polymorphonuclear leukocyte infiltration compared with the Milli-Q water group. Severe congestion and hemorrhage was also found in the NGO group. However, in the NGO + DEX group, there was less alveolar flooding and less infiltration of polymorphonuclear leukocyte compared with the NGO group. Collectively, these results suggest that DEX effectively alleviated the NGO-induced ALI.

By examining the *in vivo* biodistribution and the acute and chronic pulmonary toxicity of intratracheally instilled NGO in the lungs of mice, we demonstrated that NGO was mainly retained in the lung after intratracheal instillation and, subsequently, was slowly cleared from the lung. NGO was still present in the lung at 3 months. NGO caused dosage-dependent ALI characterized mainly by cell injury, lung edema and neutrophil infiltration. The NGO-induced ALI was progressive, as it was most severe at 48 h and was then alleviated. The NGO-induced chronic pulmonary lesions were characterized by diffuse pulmonary fibrosis. The NGO-induced ALI was related to oxidative stress and could effectively be relieved with DEX treatment.

The fact that inhaled NGO is harmful to animals might raise environmental concerns, particularly under the context that radioactive species may be carried by these carbon nanomaterials. Nanoscale, ultrafine particulates (< 100 nm in diameter) from natural and anthropogenic sources have become the cause of rapidly increasing concern.[21–24] Severe adverse health effects of inhalable ultrafine particulate matter have been demonstrated in both pulmonary toxicity and epidemiological studies.[25–27] There is a body of evidence that particulate matter can penetrate deeply into lung tissue with larger numbers and stay longer than fine or coarse particles (micrometer size or larger).[25,28] Because of their small sizes

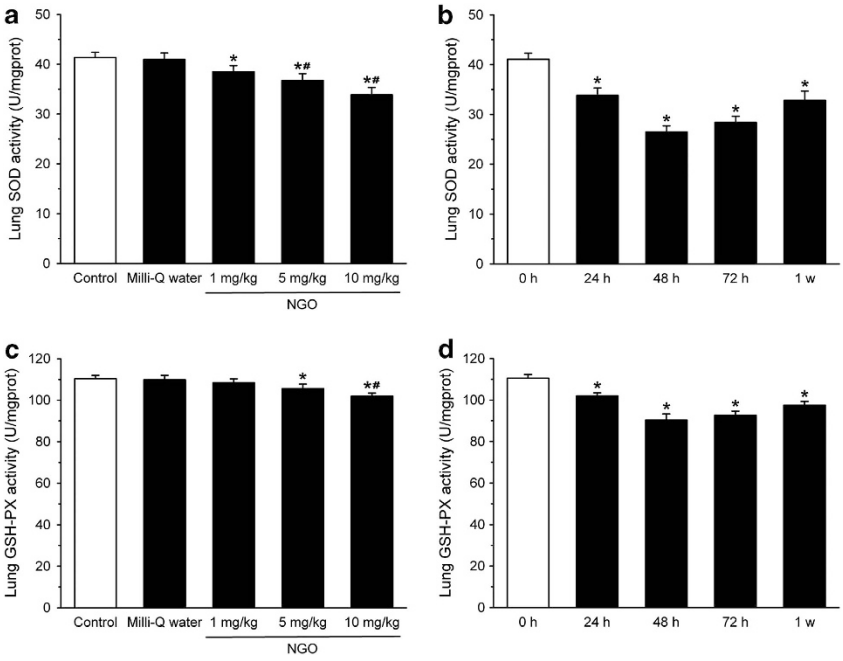

Figure 5 NGO-induced ALI is related to oxidative stress. SOD (**a**, **b**) and GSH-PX (**c**, **d**) were used as antioxidants to evaluate the degree of lung oxidative stress. (**a**, **c**) Dosage-related response. The symbol '*' indicates values that differed significantly from the control group at $P<0.05$; the symbol '#' indicates values that differed significantly from the Milli-Q water group at $P<0.05$. (**b**, **d**) Time-related response. The symbol '*' indicates values that differed significantly from the 0 h group at $P<0.05$. $N=5$ in each group. Values are presented as the mean ± s.e.m.

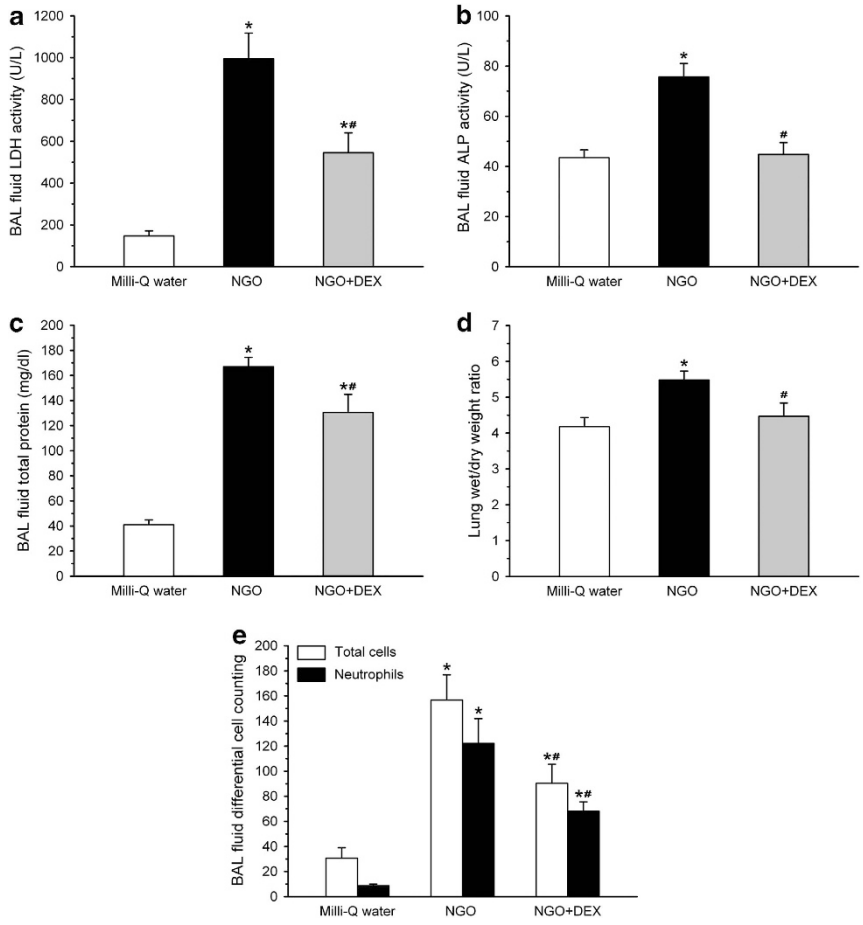

Figure 6 DEX alleviated NGO-induced ALI. (**a**–**e**) BAL fluid LDH (**a**), ALP (**b**) and total protein (**c**) assays were performed to determine the level of cell injury. The lung wet/dry weight ratio (**d**) was used to evaluate the severity of lung edema. BAL fluid differential cell counting (**e**) was used to evaluate the number and types of migrated cells. The symbol '*' indicates values that differed significantly from the Milli-Q water group at $P<0.05$; the symbol '#' indicates values that differed significantly from the NGO group at $P<0.05$. $N=5$ in each group. Values are presented as the mean ± s.e.m.

and high ratios of surface area to mass, carbon-based nanoparticulates are highly adsorptive to toxic substances, including radioactive species, which has attracted significant recent concern.[9,10,22] Given that the biodistribution of ^{125}I-NGO varies greatly from that of ^{125}I ions, it is possible that nanoparticulates can deliver radioactive isotopes deep into the lungs. These nanocarriers may also alter the biodistribution of the radioactive isotopes, settling in numerous 'hot spots' that can result in mutations and cancers. Although studies of such potential risks of radioactive nanoparticulates are still rare, the data reported here highlight the significance of protective strategies to minimize human exposure to NGO sources.[11] In addition, the possibility to reduce the NGO-induced toxicity by optimization of its sizes and surface coatings should be explored in future studies.[10,29,30]

ACKNOWLEDGEMENTS

This work was supported by the MOST 973 Program (2012CB932600), the National Science Foundation of China (No. 10775169, 10905086 and 10975179) and the CAS Innovation Program (No.095501K).

Author contributions: CF and QH conceived and designed the experiments. YZ and CP manufactured and provided the graphene oxide. BL, JY and YZ performed the experiments. BL, QH and CF analyzed the data and cowrote the paper. All authors discussed the results and commented on the manuscript.

1 Novoselov, K. S., Geim, A. K., Morozov, S. V., Jiang, D., Zhang, Y., Dubonos, S. V., Grigorieva, I. V. & Firsov, A. A. Electric field effect in atomically thin carbon films. *Science* **306,** 666–669 (2004).
2 Gong, S., Yang, C. & Qin, J. Efficient phosphorescent polymer light-emitting diodes by suppressing triplet energy back transfer. *Chem. Soc. Rev.* **41,** 4797–4807 (2012).
3 Zhang, Y., Nayak, T. R., Hong, H. & Cai, W. Graphene: a versatile nanoplatform for biomedical applications. *Nanoscale* **4,** 3833–3842 (2012).
4 Feng, L. & Liu, Z. Graphene in biomedicine: opportunities and challenges. *Nanomedicine (Lond)* **6,** 317–324 (2011).
5 Rogueda, P. G. A. & Traini, D. The nanoscale in pulmonary delivery. Part 1: deposition, fate, toxicology and effects.. *Expert. Opin. Drug. Deliv.* **4,** 595–606 (2007).
6 Kovtyukhova, N. I., Ollivier, P. J., Martin, B. R., Mallouk, T. E., Chizhik, S. A., Buzaneva, E. V. & Gorchinskiy, A. D. Layer-by-layer assembly of ultrathin composite films from micron-sized graphite oxide sheets and polycations. *Chem. Mater.* **11,** 771–778 (1999).
7 Deng, X., Yang, S., Nie, H., Wang, H. & Liu, Y. A generally adoptable radiotracing method for tracking carbon nanotubes in animals. *Nanotechnology* **19** (2008).
8 Sayes, C. M., Marchione, A. A., Reed, K. L. & Warheit, D. B. Comparative pulmonary toxicity assessments of C-60 water suspensions in rats: few differences in fullerene toxicity in vivo in contrast to in vitro profiles. *Nano Lett.* **7,** 2399–2406 (2007).
9 Oberdorster, G., Oberdorster, E. & Oberdorster, J. Nanotoxicology: An emerging discipline evolving from studies of ultrafine particles. *Environ. Health Perspect.* **113,** 823–839 (2005).
10 Gauderman, W. J., Avol, E., Gilliland, F., Vora, H., Thomas, D., Berhane, K., McConnell, R., Kuenzli, N., Lurmann, F., Rappaport, E., Margolis, H., Bates, D. & Peters, J. The effect of air pollution on lung development from 10 to 18 years of age. *N. Engl. J. Med.* **351,** 1057–1067 (2004).
11 Kaiser, J. Combining targeted drugs to stop resistant tumors. *Science* **331,** 1504–1505 (2011).
12 Ruge, C. A., Schaefer, U. F., Herrmann, J., Kirch, J., Canadas, O., Echaide, M., Perez-Gil, J., Casals, C., Muller, R. & Lehr, C. M. The interplay of lung surfactant

proteins and lipids assimilates the marcrophage clearance of nanoparticles. *PloS One* **7,** e40775 (2012).
13 Semmler-Behnke, M., Takenaka, S., Fertsch, S., Wenk, A., Seitz, J., Mayer, P., Oberdorster, G. & Kreyling, W. G. Efficient elimination of inhaled nanoparticles from the alveolar region: Evidence for interstitial uptake and subsequent reentrainment onto airway epithelium. *Environ. Health Perspect.* **115,** 728–733 (2007).
14 Shvedova, A. A., Kisin, E. R., Mercer, R., Murray, A. R., Johnson, V. J., Potapovich, A. I., Tyurina, Y. Y., Gorelik, O., Arepalli, S., Schwegler-Berry, D., Hubbs, A. F., Antonini, J., Evans, D. E., Ku, B. K., Ramsey, D., Maynard, A., Kagan, V. E., Castranova, V. & Baron, P. Unusual inflammatory and fibrogenic pulmonary responses to single-walled carbon nanotubes in mice. *J. Physiol. Lung Cell. Mol. Physiol.* **289,** L698–L708 (2005).
15 Abraham, E., Carmody, A., Shenkar, R. & Arcaroli, J. Neutrophils as early immunologic effectors in hemorrhage- or endotoxemia-induced acute lung injury. *Am. J. Physiol. Lung Cell. Mol. Physiol.* **279,** L1137–L1145 (2000).
16 Ware, L. B. & Matthay, M. A. Medical progress—the acute respiratory distress syndrome. *N. Engl. J. Med.* **342,** 1334–1349 (2000).
17 Azoulay, E., Darmon, M., Delclaux, C., Fieux, F., Bornstain, C., Moreau, D., Attalah, H., Le Gall, J. R. & Schlemmer, B. Deterioration of previous acute lung injury during neutropenia recovery. *Crit. Care Med.* **30,** 781–786 (2002).
18 Aillon, K. L., Xie, Y., El-Gendy, N., Berkland, C. J. & Forrest, M. L. Effects of nanomaterial physicochemical properties on in vivo toxicity. *Adv. Drug. Deliv. Rev.* **61,** 457–466 (2009).
19 Li, N., Xia, T. & Nel, A. E. The role of oxidative stress in ambient particulate matter-induced lung diseases and its implications in the toxicity of engineered nanoparticles. *Free Radic. Biol. Med.* **44,** 1689–1699 (2008).
20 Ding, X. M., Duan, Y. Y., Peng, C. S., Feng, H. S., Zhou, P. K., Meng, J. G., Xue, Z. Q. & Xu, Q. Z. Dexamethasone treatment attenuates early seawaters instillation-induced acute lung injury in rabbits. *Pharmacol. Res.* **53,** 372–379 (2006).
21 Nel, A. Air pollution-related illness: effects of particles. *Science* **308,** 804–806 (2005).
22 McCreanor, J., Cullinan, P., Nieuwenhuijsen, M. J., Stewart-Evans, J., Malliarou, E., Jarup, L., Harrington, R., Svartengren, M., Han, I. -K., Ohman-Strickland, P., Chung, K. F. & Zhang, J. Respiratory effects of exposure to diesel traffic in persons with asthma. *N. Engl. J. Med.* **357,** 2348–2358 (2007).
23 Oberdorster, E. Manufactured nanomaterials(Fullerenes, C-60) induce oxidative stress in the brain of juvenile largemouth bass. *Environ. Health Perspect.* **112,** 1058–1062 (2004).
24 Pope, C. A., Ezzati, M. & Dockery, D. W. Fine-particulate air pollution and life expectancy in the United States. *N. Engl. J. Med.* **360,** 376–386 (2009).
25 Brown, J. S., Zeman, K. L. & Bennett, W. D. Ultrafine particle deposition and clearance in the healthy and obstructed lung. *Am. J. Respir. Crit. Care Med.* **166,** 1240–1247 (2002).
26 Chalupa, D. C., Morrow, P. E., Oberdorster, G., Utell, M. J. & Frampton, M. W. Ultrafine particle deposition in subjects with asthma. *Environ. Health Perspect.* **112,** 879–882 (2004).
27 Marris., E. The politics of breathing. *Nature* **444,** 248–249 (2006).
28 Brown, D. M., Wilson, M. R., MacNee, W., Stone, V. & Donaldson, K. Size-dependent proinflammatory effects of ultrafine polystyrene particles: A role for surface area and oxidative stress in the enhanced activity of ultrafines. *Toxicol. Appl. Pharmacol.* **175,** 191–199 (2001).
29 Yang, K., Li, Y., Tan, X., Peng, R. & Liu, Z. Behavior and toxicity of Graphene and its functionalized derivatives in biological systems. *Small* (e-pub ahead of print 17 September 2012; doi:10.1002/smll.201201417).
30 Duch, M. C., Budinger, G. R. S., Liang, Y. T., Soberanes, S., Urich, D., Chiarella, S. E., Campochiaro, L. A., Gonzalez, A., Chandel, N. S., Hersam, M. C. & Mutlu, G. M. Minimizing oxidation and stable nanoscale dispersion improves the biocompatibility of graphene in the lung. *Nano Lett.* **11,** 5201–5207 (2011).

Supplementary Information accompanies the paper on the NPG Asia Materials website (http://www.nature.com/am)